Analysis of linear and angular errors of a small coordinate measuring machine (SCMM)

J. Loh, J. McBride, M. Hill & D. Zhang
Electro-Mechanical Research Group, University of Southampton, U.K.

Abstract

In this research, a small coordinate measuring machine has been assembled using standard opto-mechanical parts, 3 precision carriages and a Keyence LT-8010 laser displacement measuring probe. A study was conducted to assess the positioning accuracy of this machine by employing laser interferometry principles to measure error components of individual positioning carriages. An error model of the small coordinate measuring machine was also developed to take into account these error components and compute the resulting positioning capabilities of this machine. From the analysis of linear and angular errors, it became clear that after 3 years of operation, the positioning carriages had developed faults that were affecting their normal working abilities. This research concludes by analysing the errors obtained from the measurement of the individual positioning carriages and determining possible causes for these errors.

1. Introduction

A systematic approach to the analysis of CMM errors and a representation of their influences is critical to correct these errors and improve the performance of a CMM. This can be achieved through error modelling. In Figure 1, the position errors of a carriage have been shown described by three displacement errors and three rotational errors around its axis of motion. The carriages of any CMM or machine tool are components that provide movement between a measurement probe and the measured object. Guideways within these carriages constrain motion in any direction other than a specific linear or angular path of travel. The location along the remaining 'free' path is then constrained by an actuator, often a motor-driven ballscrew/nut combination, which positions the carriage to a given encoder determined location. However, the motion of the carriage is often not ideal. There are undesirable accompanying rotational errors and translation errors

(such as straightness errors) due to manufacturing imperfections of the positioning carriages and the fitting of encoder's scales. As it moves, the carriage may rotate by small angles, and/or be displaced by small amounts in the two dimensions perpendicular to the ideal carriage path. These displacement errors, δy and δz can be caused by guideway imperfections. Additionally, a third small displacement error, δx, along the ideal path is often attributed to manufacturing errors, thermal expansion of the scale and other machine components, such as the ballscrew etc.

From the basic kinematics of a constrained rigid body, errors exist in linear or rotational motions associated with each degree of freedom (DOF). With multiple carriages, there are squareness errors associated with the mechanical alignment of a pair of carriages. A three-axis coordinate measurement machine therefore has twenty-one rigid body error components: each axis possessing three linear errors, three rotational errors and a squareness error [1]. The squareness error refers to the orthogonal alignment error of a pair of carriage, e.g. x and y, or y and z carriages.

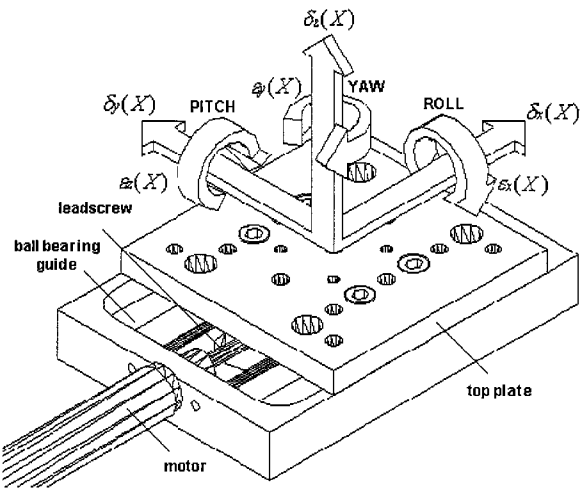

Figure 1: Error components of a positioning carriage

2. Mathematical modelling

Modelling a CMM is essential to establish a generalised framework that facilitates a systematic approach to the analysis of errors. The framework can be applied to the assessment of the influence of errors on the overall accuracy of a multi-axis machine [2]. Multi-axis machines are typically composed of a sequence of elements connected by joints that provide either translational or rotational motion, closely resembling the kinematics of a robot. Kinematics describes the relationship between the positions, velocities, and accelerations of the links of a manipulator, where a manipulator is an arm, finger, or leg. A mathematical framework becomes useful for describing the relationships of the various joints in a robot to, for example, the end effector at the end of the kinematic chain. A

CMM can be considered as an open chain mechanism and this technique of modelling has roots that can be traced in the literature of robotics [3].

The Denavit and Hartenberg modelling approach proposed a systematic notation for assigning right-handed orthonormal coordinate frames, one to each link in an open kinematic chain of lines [4]. The base and each link i of the chain are assigned to a specific frame K_i, which is fixed to the link. The position and orientation of a link frame changes with respect to a neighbouring link frame according to the motion of their connecting joint. Therefore coordinate frame K_i can be described from its precedent link frame K_{i-1} by means of a homogeneous transformation. This homogeneous transformation includes the joint angle (for rotary joints) or the joint offset (for prismatic joints). With a 4 x 4 homogeneous transformation matrix (HTM), the fundamental operations of translation and rotation can be represented in a single matrix with reference to the origin of the original coordinate frame.

Finally the end effector frame K_n can be transformed to the base frame by multiplication of the entire link transformations through the kinematic chain. So in order to transform any position/orientation relative to the tool frame (e.g. by sensors attached there) to the base frame (e.g. where it is fixed to the floor), the sorted sequence of homogeneous transformations from tip to toe via K_{i-1}, K_{i-2}, ... , K_0 has to be processed. The remaining task is to set up all the homogeneous transformation matrices for a particular type of kinematic chain, considering geometrical attributes of link arrangements and types of joints.

2.1 Coordinate frame assignment

Once the link-attached coordinate frames have been assigned to the various links of the CMM, each axis of the CMM relative to one another and to the reference frame can be modelled. A diagram of the coordinate frames 'attached' to the SCMM has been illustrated in Figure 2. For simplification purposes, small angle approximation of the errors is applied to the mathematical model and only first order terms of error equations are considered. These approximations have been commonly applied towards a generalised modelling of kinematic errors [4]. A HTM is of the general form as follows:

$$ {}^{x}T_{y} = \begin{bmatrix} R_{1x} & R_{2x} & R_{3x} & P_x \\ R_{1y} & R_{2y} & R_{3y} & P_y \\ R_{1z} & R_{2z} & R_{3z} & P_z \\ 0 & 0 & 0 & 1 \end{bmatrix} \equiv \begin{bmatrix} Rotation & Position \\ Perspective & Scale \end{bmatrix} \quad (1) $$

where R and P represent the orientation and position of a coordinate frame with respect to another coordinate frame, respectively. The matrix that is represented by ${}^{x}T_{y}$ exemplifies a transformation of coordinate frame x into frame y. The combination of all elements of the HTMs can then be used to build a mathematical model. This model would enable the calculation and prediction of the resultant

error vector at the probe-workpiece interface for error compensation. The resultant error motion of a carriage is a combination of rotational and translational errors [5]. The HTMs of rotational (T_{rot}) and translational (T_{trans}) errors are:

$$T_{rot} = \begin{bmatrix} 1 & -\varepsilon_z & \varepsilon_y & 0 \\ \varepsilon_z & 1 & -\varepsilon_x & 0 \\ -\varepsilon_y & \varepsilon_x & 1 & 0 \\ 0 & 0 & 0 & 1 \end{bmatrix}, \quad T_{trans} = \begin{bmatrix} 1 & 0 & 0 & \delta_x \\ 0 & 1 & 0 & \delta_y \\ 0 & 0 & 1 & \delta_z \\ 0 & 0 & 0 & 1 \end{bmatrix} \tag{2}$$

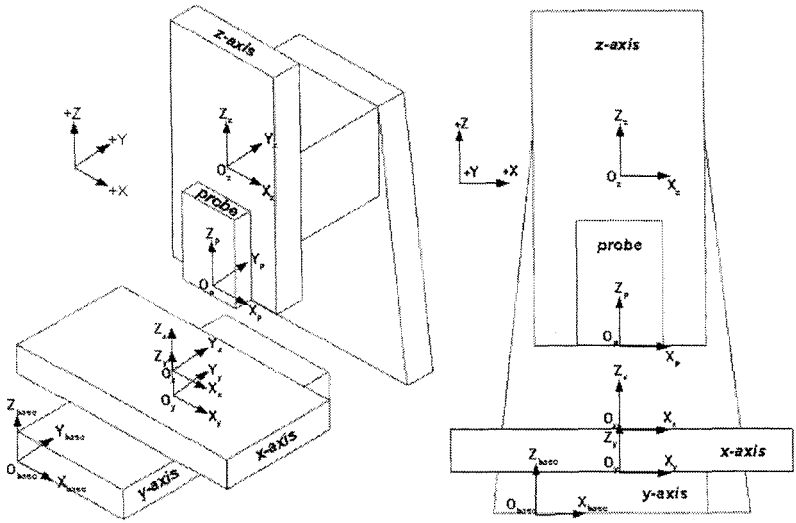

Figure 2: Coordinate frames of the SCMM

where ε_x (roll), ε_y (pitch), ε_z (yaw) are rotational errors about x, y, and z axes and δ_x, δ_y and δ_z represent translational errors along the three axes respectively as previously shown in Figure 2. The general forward kinematics based error form for any intrinsic machine is based on the physical relationships of the machine parts and can be represented by this equation:

$$[P_a] = [P_i] + [E] \tag{3}$$

where $[P_a]$ and $[P_i]$ describes the actual position (real) and ideal (nominal) position of the probe. The combination of rotational and translational errors would provide a resultant HTM describing the error, $[E]$ in position of the nominated axis with respect to its ideal position is:

$$E = T_{rot}T_{trans} = \begin{bmatrix} 1 & -\varepsilon_z & \varepsilon_y & \delta_x \\ \varepsilon_z & 1 & -\varepsilon_x & \delta_y \\ -\varepsilon_y & \varepsilon_x & 1 & \delta_z \\ 0 & 0 & 0 & 1 \end{bmatrix} \tag{4}$$

2.2 Transformation of coordinate frames

The base coordinate reference, which represents the machine origin, provides the initiating point for the transformation process. From this reference position, any point in space within the working volume of the SCMM can be clearly specified. The reference frame, also known as the base frame, $\boldsymbol{O}_{base}$, is particularly assigned for the purpose of calibration covering the working zone of this machine. There are four more independent coordinate systems, namely $\boldsymbol{O}_y$ for the y carriage, $\boldsymbol{O}_x$ for the x carriage, $\boldsymbol{O}_z$ for the z carriage, $\boldsymbol{O}_p$ for the probe coordinate frame. Referring back to Figure 2, the y carriage sits on a stable base, and therefore is the initial reference to the base coordinate system. Any error variables that are related to the y carriage are tagged with a *(Y)*. For example, $\varepsilon_x(Y)$ refers to the roll rotational error about the y carriage. The actual position and orientation of y carriage (y) in the base coordinate system (*base*) can be represented in the following form:

$$\left[{}^{base}T_y\right]_{Actual} = \begin{bmatrix} 1 & -\varepsilon_z(Y) & \varepsilon_y(Y) & \delta_x(Y)+a(Y) \\ \varepsilon_z(Y) & 1 & -\varepsilon_x(Y) & y+\delta_y(Y)+b(Y) \\ -\varepsilon_y(Y) & \varepsilon_x(Y) & 1 & \delta_z(Y)+c(Y) \\ 0 & 0 & 0 & 1 \end{bmatrix} \tag{5}$$

$\varepsilon_x(Y)$, $\varepsilon_y(Y)$, $\varepsilon_z(Y)$ - *rotational errors of y-axis*
$\delta_x(Y)$, $\delta_y(Y)$, $\delta_z(Y)$ - *translational errors of y-axis*
$a(Y)$, $b(Y)$, $c(Y)$ - *constant offset in x, y and z direction between* O_{base} *and* O_y
y - *travel distance along y-axis*

Next, the actual position and orientation of x-axis ($\boldsymbol{O}_x$) in y-axis coordinate system ($\boldsymbol{O}_y$) can be defined:

$$\left[{}^{y}T_x\right]_{Actual} = \begin{bmatrix} 1 & -\varepsilon_z(X) & \varepsilon_y(X) & x+\delta_x(X)+\alpha_{xy} \\ \varepsilon_z(X) & 1 & -\varepsilon_x(X) & \delta_y(X) \\ -\varepsilon_y(X) & \varepsilon_x(X) & 1 & \delta_z(X)+c(X) \\ 0 & 0 & 0 & 1 \end{bmatrix} \tag{6}$$

$\varepsilon_x(X)$, $\varepsilon_y(X)$, $\varepsilon_z(X)$ - *rotational errors of x-axis*
$c(X)$ - *constant offset in z direction between* O_y *and* O_x
$\delta_x(X)$, $\delta_y(X)$, $\delta_z(X)$ - *translational errors of x-axis*
α_{xy} - *squareness error between the x and y-axes*
x - *travel distance along x-axis*

As well as the actual position and orientation of z-axis ($\boldsymbol{O_z}$) in x-axis coordinate system ($\boldsymbol{O_x}$):

$$\left[{}^{x}T_{z}\right]_{Actual} = \begin{bmatrix} 1 & -\varepsilon_z(Z) & \varepsilon_y(Z) & \delta_x(Z)+\alpha_{xz}+a(Z) \\ \varepsilon_z(Z) & 1 & -\varepsilon_x(Z) & \delta_y(Z)+\alpha_{yz}+b(Z) \\ -\varepsilon_y(Z) & \varepsilon_x(Z) & 1 & z+\delta_z(Z)+c(Z) \\ 0 & 0 & 0 & 1 \end{bmatrix} \tag{7}$$

$\varepsilon_x(Z)$, $\varepsilon_y(Z)$, $\varepsilon_z(Z)$ - *rotational errors of z-axis*
$a(Z)$, $b(Z)$, $c(Z)$ - *constant offset in x, y and z direction between O_x and O_z*
$\delta_x(Z)$, $\delta_y(Z)$, $\delta_z(Z)$ - *translational errors of x-axis*
α_{xz}, α_{yz} - *squareness error between the x and z-axes and y and z-axes*
z - *travel distance along z-axis*

And lastly the actual position and orientation of *probe* ($\boldsymbol{O_P}$) in z-axis coordinate system ($\boldsymbol{O_z}$):

$$\left[{}^{z}T_{p}\right]_{Actual} = \begin{bmatrix} 1 & -\varepsilon_z(P) & \varepsilon_y(P) & a(P) \\ \varepsilon_z(P) & 1 & -\varepsilon_x(P) & b(P) \\ -\varepsilon_y(P) & \varepsilon_x(P) & 1 & c(P) \\ 0 & 0 & 0 & 1 \end{bmatrix} \tag{8}$$

$\varepsilon_x(P)$, $\varepsilon_y(P)$, $\varepsilon_z(P)$ - *rotational errors of probe*
$a(P)$, $b(P)$, $c(P)$ - *constant offset in x, y and z direction between O_z and O_p*

3. Diagnosis of error components

The Renishaw Performance Measurement system was used in the diagnosis of errors in each of the carriages of the SCMM [6]. The Renishaw Performance Measurement system has been used with the aid of a Renishaw trained technician. The standard linear interferometer test has been employed in the following test and this test follows the strict guidelines of the ISO-10360 (CMM) standard and determines the accuracy and repeatability of positioning in numerically controlled axes. A set of fixed optics (or reflector) is mounted on the base of the SCMM. An additional set of moving optics is magnetised on the top plate of the y carriage. By moving the y carriage, stopping and dwelling at constant positional intervals, interferometric displacements of the actual motion can be collected from the Renishaw system and compared with the desired values. The difference between these two values would constitute a linear error in the corresponding carriage.

3.1 Results of linear tests

The results of the linear test conducted on the x, y and z-carriages of the SCMM were obtained. As error characteristics of the y- and z-carriages were found to be somewhat similar, the discussion starts with these two sets of errors, and is followed by that of the x-carriage. These errors are plotted in Figure 3. From these plots, it can be clearly seen that the linear errors were increasing, but in the negative direction. This is an indication of 'under-travel' and means that the carriage did not reach its desired position. 'Over-travel', on the other hand, refers to the carriage coming to rest past its desired position.

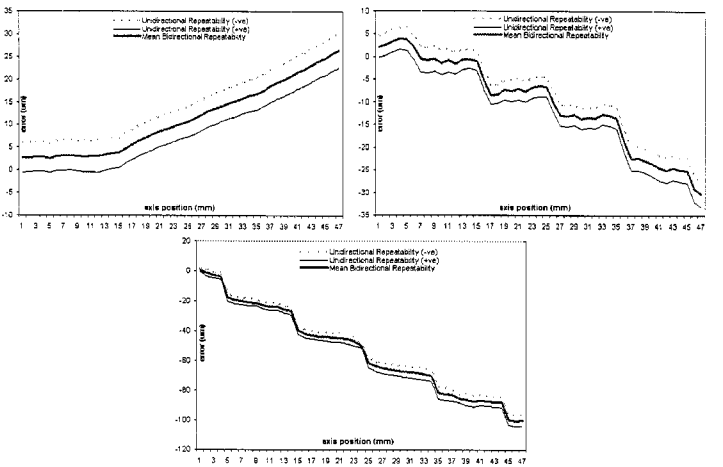

Figure 3: Linear errors for x(top left), y(top right), z(bottom centre) carriages

3.2 Results of angular errors – yaw and pitch

Angular errors, namely roll, pitch, and yaw, result from any deviation in motion along an axis by an angle of rotation around one of three axes. The angular interferometric tests were carried out in the same manner as the linear test, except that specialized angular optics was used instead. From the interferometer tests, the roll errors were found to be negligible based on the recommendations from the Renishaw technician present and therefore only the pitch and yaw errors were investigated. This resulted in a remaining total of six sets of angular errors, plotted as Figure 4 and 5. The angular yaw and pitch errors of all three carriages of the SCMM were shown to possess the periodic ripple characteristics which were observed in the linear errors as well. All these errors obtained presented an interesting account to be debated in the next section, which will collate the collected information regarding these three carriages and attempt to analyse these errors in a logical manner.

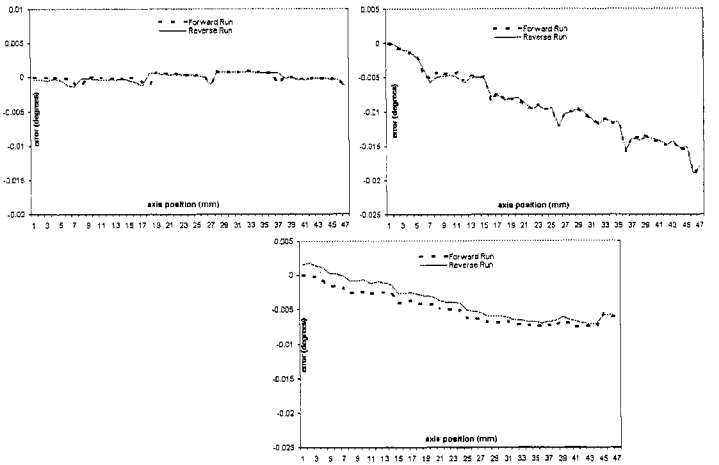

Figure 4: Angular yaw errors for x(top left), y(top right), z(bottom centre) carriages

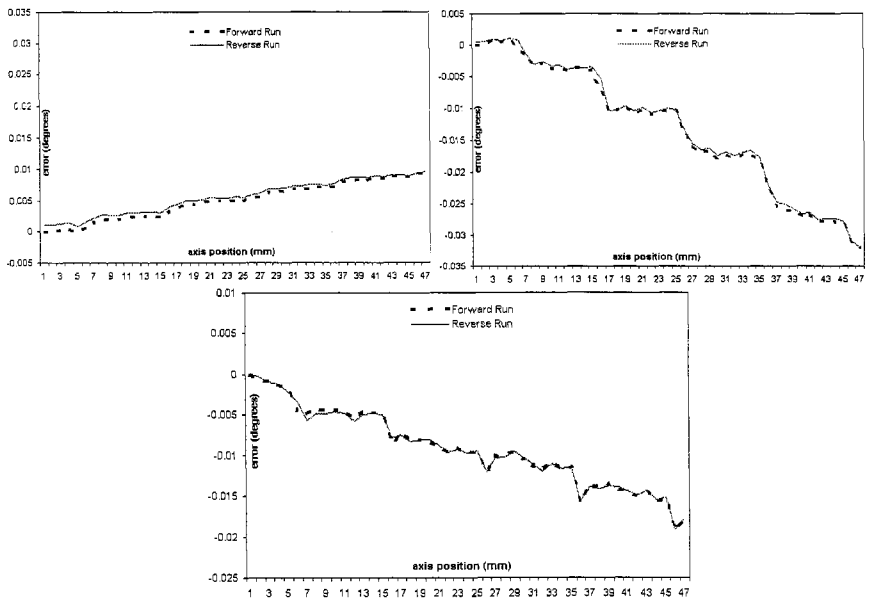

Figure 5: Angular pitch errors for x(top left), y(top right), z(bottom centre) carriages

4. Error analysis

Based on the linear and angular errors of the three carriages that were discussed in the previous sections, an investigation of the operating characteristics of the

carriages used in the SCMM revealed the following causes that may be attributed to the linear and rotational errors. Some of the following possible causes were suggested by the manufacturer of the carriages and these include:

i. The leadscrew of the carriage is the rotating mechanism providing the linear motion. It came supplied with a flat tip end, with an additional interchangeable ball tip. The leadscrew has direct contact with the driven plate which moves the top plate. In the event of a misalignment problem of the leadscrew with the driven plate, a helical oscillatory leadscrew motion could be transferred to the driven plate. This was the main cause of the ripple behaviour seen in the linear and angular errors and users of similar carriages have reported the same problem.

ii. The high precision ball-bearing guides of the carriages could lose their accuracy and smoothness of operation through wear and tear. If the carriage had been subjected to a sudden impact, this could also damage the ball bearings. Assuming that one or more ball bearings had lost their roundness, this could translate to an oscillatory behaviour. All the carriages of the SCMM have been in operation for more than two years. Out-of roundness characteristics of the ball bearings could result in the periodic 'ripple' error characteristics seen in the linear and angular test results.

iii. A grub screw that holds the leadscrew firmly in position on the frame of the stage was found to be 'over-torqued'. The additional torque may have unnecessarily 'compressed' the leadscrew. The translated motion from the leadscrew would therefore be not as fine and smooth. If this is not properly dealt with, it might deform the leadscrew permanently.

iv. Movements of the carriages might be impeded if there is any foreign dirt and dust accumulated in the leadscrew or guideways. These should be cleaned and lubricated regularly. The carriages have been in operation for a few years and even under a metrology controlled environment, dust and dirt could be present.

5. Error modelling

In order to determine the actual coordinates of the probe at a point in space, a series of transformations of the matrices can be carried out. The transformation matrix of the probe with respect to the base reference frame is therefore given by:

$$T_{probe} = {}^{base}T_p = {}^{base}T_y \, {}^{y}T_x \, {}^{x}T_z \, {}^{z}T_p \tag{9}$$

Using MATLAB 5.3, the resultant matrix T_{probe} can be easily worked out. From the matrix T_{probe}, the position vectors of the probe $[P_x, P_y, P_z]$ can be extracted and is of the following form:

$$Px = x + a(P) + [\delta_x(X)+\delta_x(Y)+\delta_x(Z)] + [\alpha_{xy}(Y)+\alpha_{xz}(Z)] + [\varepsilon_y(X)+\varepsilon_y(Y)] * z - [\varepsilon_z(X)+\varepsilon_z(Y)+\varepsilon_z(Z)] * b(P) + [\varepsilon_y(X) + \varepsilon_y(Y) + \varepsilon_y(Z)] * c(P);$$

$$Py = y + b(P) + [\delta_y(X)+\delta_y(Y)+\delta_y(Z)] + \alpha_{yz}(Z) - [\varepsilon_x(X)+\varepsilon_x(Y)] * z + [\varepsilon_z(X)+\varepsilon_z(Y)+\varepsilon_z(Z)] * a(P) - [\varepsilon_x(X)+\varepsilon_x(Y)+\varepsilon_x(Z)] * c(P) + \varepsilon_z(Y) * x;$$

$$Pz = z + c(P) + [\delta_z(X)+\delta_z(Y)+\delta_z(Z)] - [\varepsilon_y(X)+\varepsilon_y(Y)+\varepsilon_y(Z)] * a(P) + [\varepsilon_x(X)+\varepsilon_x(Y)+\varepsilon_x(Z)] * b(P) - \varepsilon_y(Y) * x; \quad (10)$$

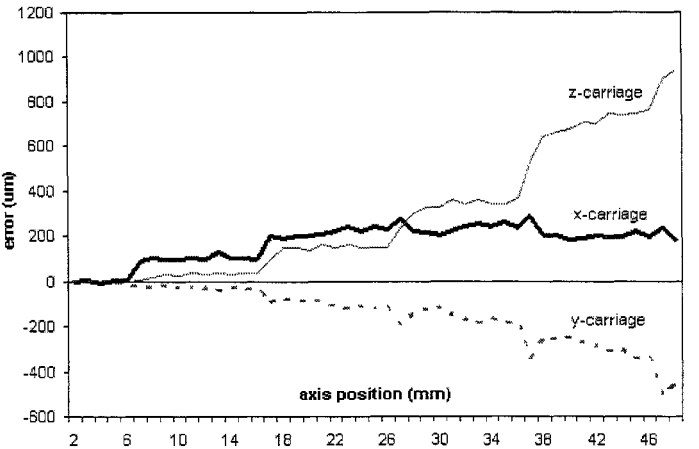

Figure 6: Positioning errors in x, y and z

The coordinates $[P_x, P_y, P_z]$ describe the ***actual*** position of the probe with respect to the base coordinate system. The ideal position of the probe is the position or the set of coordinates where the probe is assumed to be. With the actual position of the probe calculated and the ideal position known *apriori*, the error in the position of the sensor can thus be calculated and therefore be the difference in position, if any, between P_{actual} and P_{ideal}.

From the positioning errors of the three carriages shown in Figure 6, the assembly flaws and operating nature of the rotating leadscrew and guideways of the carriages of the SCMM have contributed significantly to the overall positional error of the probe. Consistent periodic 'ripples' can be found in Figure 6 through the entire range of travel in each of the three carriages. The first initial 6*mm* of travel for all three carriages were quite 'error-free', but subsequent movements resulted in the repeatable 'V-grooves'. These V-grooves were found to be consistently repeated over cumulative travel distances of 10*mm*.

This has a serious impact on the ability of the carriages to position accurately. The use of a ball-bearing tip for the leadscrew is essential to try and eliminate this error. In the case of the *z*-carriage, it must be reiterated that the combined weight of the probe and its associated mechanical structure do have a bearing on the magnitude of the errors. Errors of the *z* carriage are up to 5 times that of the other two lateral carriages. The weight borne by the *z* carriage should be reduced through use of lighter structural components or a bridge-type

configuration. The remaining errors that cannot be eliminated through re-design must be compensated using software corrections.

6. Conclusion

From the above discussion, the importance of calibrating a CMM and analysing the errors obtained from the calibration process has been demonstrated. Based on the different sets of errors, it became possible to predict the type of faults that was developing within the machine. These faults can be quickly resolved to ensure that subsequent machine operation can be 'error-free'. This consequently boosts the confidence of the end-user by partially eliminating mechanical errors that are attributed to the physical assembly of the CMM parts. In performing the laser interferometry measuring exercise, this also sets out as the basis for obtaining the error components that will be necessary to model the kinematic and geometric errors of the Small Coordinate Measuring Machine. A further development of the small CMM employs significantly improved positioning carriages and this, along with other improvements, has led to a much more accurate measurement system [7].

References

1. Barakat, N.A. and M.A. Elbestawi. *Detection, modelling and compensation of geometric errors in coordinate measuring machines*. Proceedings of the ASME Manufacturing Science and Engineering Division. 1998: p. 597-603.
2. Eman, K., B. Wu, and M. DeVries, *A generalized geometric error model for multi-axis machines*. Annals of the CIRP, 1987. **36**: p. 253-256.
3. Craig, J., *Introduction to robotics and mechanics control*. 1989, Reading, MA: Addison-Wesley.
4. Barakat, N.A., M.A. Elbestawi, and A.D. Spence, *Kinematic and geometric error compensation of a coordinate measuring machine*. International Journal of Machine Tools & Manufacture, 2000. **40**: p. 833-850.
5. Barakat, N.A., A.D. Spence, and M.A. Elbestawi, , (), *Adaptive compensation of quasi-static errors for an intrinsic machine*. International Journal of Machine Tools and Manufacture, 2000. **40**: p. 2267-2291.
6. Renishaw-plc-UK, *http://www.renishaw.co.uk*, 2002.
7. Taicaan Technologies www.taicaan.com.